Plant Physiology and Biochemistry 196 (2023) 859–867

Contents lists available at ScienceDirect

Plant Physiology and Biochemistry

journal homepage: www.elsevier.com/locate/plaphy

Effect of nanobiochar (nBC) on morpho-physio-biochemical responses of black cumin (*Nigella sativa* L.) in Cr-spiked soil

Musarrat Ramzan [a,*], Arooj Zia [a], Gul Naz [b], Muhammad Shahid [c], Anis Ali Shah [d], Ghulam Farid [e]

[a] Department of Botany, Faculty of Chemical and Biological Sciences, The Islamia University of Bahawalpur, Pakistan
[b] Institute of Physics, Faculty of Physical and Mathematical Sciences, The Islamia University of Bahawalpur, Pakistan
[c] Cholistan Institute of Desert Studies, The Islamia University of Bahawalpur, Pakistan
[d] Department of Botany, Division of Science and Technology, University of Education, Lahore, Pakistan
[e] Nuclear Institute of Agriculture and Biology, Faisalabad, Pakistan

ARTICLE INFO

Handling Editor: Shivendra Sahi

Keywords:
Antioxidant enzymes
Chromium
Nanobiochar
Nigella sativa
Oxidative stress

ABSTRACT

Chromium is a highly toxic heavy metal. High concentrations of Cr (III) can affect metabolic processes in plants, resulting in different morphological, physiological, and biochemical defects. Agricultural practices such as sewage irrigation, over-fertilization, and sewage sludge application contribute significantly to Cr contamination. It can reduce the growth of plants by affecting the activity of antioxidant enzymes. The materials in nano form play an important role in nano-remediation and heavy metals absorption due to their high surface area and micropores. This research was conducted to study the potential of foliar application of nanobiochar/nBC (100 mg/L^{-1} and 150 mg/L^{-1}) for mitigation of Cr (III) stress (200 mg/kg and 300 mg/kg) in black cumin (*Nigella sativa*) plants. The results showed that increased Cr stress (300 mg/kg) decreased the plant growth parameters, chlorophyll content, total soluble sugars, and proteins. However, increased the level of hydrogen peroxide (H_2O_2) and malondialdehyde acetate (MDA) as a result of the activity of antioxidant enzymes (Catalase, Superoxide dismutase, peroxidase dismutase, and ascorbic peroxidase) increased in *Nigella sativa* seedlings. Foliar application of the nBC (100 mg/L^{-1}) increased plant growth parameters, chlorophyll content, and osmoprotectants, while decreasing the levels of oxidative stress markers (H_2O_2 and MDA). Furthermore, with the application of nBC, the antioxidant enzyme activity considerably improved. Improved antioxidant activity shows that nBC helped to decrease oxidative stress, which in return improved the growth of *Nigella sativa* seedlings. Overall, present study findings concluded that foliar application of nBC in *Nigella sativa* seedlings improved growth, chlorophyll, and antioxidant enzymes. The nBC treatment of 100 mg/L^{-1} showed better results compared to 150 mg/L^{-1} under chromium stress.

1. Introduction

Nigella sativa L. is an annual herb in the Ranunculaceae family that produces primarily in various regions of southern Europe and Asia (Hosseini et al., 2012), including Turkey, Syria, Saudi Arabia, India, and Pakistan (Rajasekhar and Kuldeep, 2011). Black cumin, known as a Haba al-Barakah (blessed seed) or wonder herb, was regarded as "the herb from the heaven" by ancient herbalists (Ahmad et al., 2013). "This black cumin is curative for all diseases except death," The Prophet Mohammad (PBUH) once said (Sahih Al-Bukhari, Book 76, Hadith 10), As a result, it is referred to as 'Prophetic medicine' throughout the Muslim community. Black cumin has been prescribed in traditional medical systems such as Unani, Tibb, Ayurveda, and Siddha, and is used to treat a variety of diseases and ailments in Arab nations, Africa, Asia, and Europe, including asthma, rheumatism, bronchitis, headache, inflammation, back pain, paralysis, and hypertension (Ali et al., 2018). *Nigella sativa* is normally used to treat toxicity of Cd in animals (Kishwar et al., 2016; Kishwar and Anwar, 2012; Kanter et al., 2005; El-Dakhakhny et al., 2002). The primary volatile component of seeds is thymoquinone (Yimer et al., 2019; El-Dakhakhny et al., 2002; Badary et al., 2003), which have antioxidant properties and aid in the treatment of Cd toxicity in animals. Tolerance to heavy metals enhanced in many

* Corresponding author.
E-mail address: musarrat.ramzan@iub.edu.pk (M. Ramzan).

https://doi.org/10.1016/j.plaphy.2023.02.037
Received 27 September 2022; Received in revised form 21 January 2023; Accepted 21 February 2023
Available online 23 February 2023

crops by Chelation (Abbas et al., 2020), different plant extracts used for foliar application (Danish et al., 2019a,b; Allah Ditta et al., 2021) and the use of rhizobacteria that promote plant growth (Islam et al., 2016; Stambulska et al., 2018; Danish et al., 2019a,b).

Chromium is the seventh most common chemical element on the earth, and mined in India, Kazakhstan and South Africa (Shahid et al., 2017; USGS, 1996–2021). Cr is major pollutant that enters soil by anthropogenic activity and geological processes (Coetzee et al., 2020; Jaishankar et al., 2014; Rajapaksha et al., 2013). It has been reported that Cr is released into the agricultural soil in China through sewage irrigation, fertilizers, livestock manure, and sewage sludge (Peng et al., 2019). However, overused of chemical fertilizers and pesticides slowly caused Cr pollution in agricultural lands (Gill et al., 2013; Javed et al., 2021). Chromium has 0 to VI valence states. The most toxic state for plants, animals, and humans is Cr (VI) (Medda and Mondal, 2017; Pavesi and Moreira, 2020; Jan et al., 2020). Despite the fact that Cr(III) is an essential element for humans and has been related to carbohydrate, lipid, and protein metabolism, human health issues are concentrated on Cr toxicity, overexposure and consumption of which causing harm to humans (e.g., kidneys, skin, lungs and liver) (Zhao et al., 2020; Pavesi and Moreira, 2020). Moreover, because chromium is quickly absorbed in the food system, humans are largely exposed to it through soil-crop system (Christou et al., 2021; EFSA Panel on Contaminants in the Food Chain, 2015). Cr exposure in high concentration have damaging effects on biochemical and physiological attributes of the plants (Kapoor et al., 2022; Khattak et al., 2021; Stambulska et al., 2018). High level of Cr in the soil can cause a delay in seed germination (Hafiz and Ma, 2021; Medda and Mondal, 2017), harm ecosystem of the soil and inhibit growth of the plants (Dazy et al., 2008). Several reports have shown that Cr toxicity is an effective photosynthesis inhibitor in plants (Basit et al., 2022; Wang et al., 2013). Chlorophyll content reductions initiated by Cr stress observed in a variety of plants, including *Taxiphyllum taxirameum, Cicer arietinum, Hibiscus esculentus* L., and *Brassica napus* L. (Chen et al., 2018c; Medda and Mondal, 2017; Amin et al., 2013; Najafian et al., 2012).

Researchers are very interested in biochar ammendment because of its potential to eliminate pollutants, reduce the changes in climate, and promote growth of the plant as well as the quality of the soil. (Lehmann et al., 2015; Alimohammadi et al., 2011; Tripathi et al., 2011; Ashfaq et al., 2017; Khodakovskaya et al., 2013). Nanoremediation has become extremely important in pollution prevention, environmental improvement, and the identification and remediation of pollutants such as heavy metals and organic compounds. The nanomaterials improves absorption of heavy metals because of their high surface area, large micropores, and microinterface. As a result, nanomaterials with environmental benefits are gaining popularity (Liu et al., 2020). Biochar particle sizes range from micrometres to centimetres depending on pyrolysis method (Lehmann et al., 2015). Further reducing the particles size of the biochar to the nanoscale range improved their characteristics (Naghdi et al., 2019; Sulaiman et al., 2013; AkilaKesavan, 2014; Naghdi et al., 2017). The particles of nanobiochar (nBC) has ability to absorb pollutants that includes heavy metals, herbicides, polycyclic aromatic hydrocarbons and polychlorinated biphenyls (Wang et al., 2013). Yue et al. (2019) examined nBC for lowering oxidative stress and metal toxicity (Cd^{2+}) in rice seedlings and discovered a substantial reduction in Cd^{2+} toxicity and oxidative stress. The concentration of Cd in *Brassica chinensis* L. was lowered with nBC treatment than in untreated soil groups ($P < 0.05$) (Liu et al., 2020).

The primary objective of this study was to assess the effect of exogenous nBC on growth, photosynthetic pigments, oxidative stress biomarkers, antioxidant machinery in *N. sativa* under Cr-stress. Moreover, we investigated the efficiency of foliar nBC management in plant defense response under Cr-stress. Black cumin is an herbal spice and used in Asian foods and pickles but it is highly sensitive to Cr-stress. We hypothesized that foliar application of nBC may improve growth in *N. sativa* through modulation of key physiochemical processes under different levels of Cr-spiked soil. To the best of our knowledge, this is the first study to investigate the role of foliar application of nBC for mitigating Cr stress in *Nigella sativa* seedlings.

2. Materials and methods

2.1. Preparation of biochar and nano-biochar

In this study, sugarcane pressmud was used to make nBC, which was subsequently employed as an amendment. Saxena et al. (2014) method was used for the preparation of nBC. The prepared biochar was carefully ground and sieved (2 mm) to achieve fine particles. Thoroughly mixed 1 g of powdered biochar with 1000 mL of water, stirred for 30 min and let it sit. The supernatant was transferred to filter paper for filtering while the pellet was discarded. After filtration, it was washed twice to remove any residue. The filtrate was dried in the oven at 60 °C for 5 h and placed in the incubator at 120 °C for 5 h to dry further. The dried nBC's characterization was performed for its structure and composition. The nBC solutions of 100 mg/L^{-1} and 150 mg/L^{-1} (Liu et al., 2020) were prepared for foliar application.

2.2. Characterization of nanobiochar

The absorption spectrum of nBC sample was obtained via an Epoch Microplate Spectrophotometer in the wavelength ranging from 300 nm to 700 nm. For structural investigation, the X-ray diffraction (XRD) for this sample was carried out through Bruker-D8 Advance X-ray Diffractometer with Cu *Kα* radiation (λ = 1.54 Å), operated at 35 mA and 40 KeV. For analyzing the morphology of nBC sample, a ZEISS SEM microscope set to 15 kV accelerating voltage was utilized.

2.3. Experimental design

The experimental plant was black cumin (*Nigella sativa*). Viable seeds were chosen and used in the greenhouse experiment. Chromium was purchased from the Sigma-Aldrich. For further experimentation, different concentrations of Cr were prepared. The experiment was held at the Department of Botany and Cholistan Institute of Desert Studies, The Islamia University of Bahawalpur. For the greenhouse experiment, the soil was collected from a local nursery in Bahawalpur and sieved with a 2 mm steel sieve. The chromium was introduced into the soil in the form of chromium (III) nitrate nonahydrate ($Cr(NO_3)_3{\cdot}9H_2O$). The soil was spiked with 200 mg/kg and 300 mg/kg Cr by using the previously described method (Ramzan et al., 2022), whereas the unspiked soil was used as a control. To achieve the right balance between the solid and liquid phases of the soil, contaminated soils were kept in the shade for a month before seed sowing. The experiment was conducted using a completely random design (CRD). Each treatment consists of three replicates. Average 15–30 °C temperature, 65–75 relative humidity, 16 h day/8 h night photoperiod were maintained in the greenhouse for single growing season.

2.4. Application of nanobiochar

Seeds were planted in seedling trays. After 22 days of sowing, the seeds began to germinate. When the seedlings attained the desired height after 3 weeks of germination, 6 to 8 seedlings were transplanted per pot at equal distances. After two weeks of transplantation, plants were thinned and foliar application of the first treatment of nanobiochar (100 mg/L^{-1} and 150 mg/L^{-1}) was given. The second and third treatments were given one week interval. To maintain 40% moisture in all pots, the plants were irrigated when required. The plant height was measured, and the number of surviving plants was recorded. All plants were cultivated until certain plants reached a constant height.

2.5. Estimation of plant growth attributes

After 40 days of transplantation, the plants were harvested and cut into two parts viz., Root and Shoot. The random sampling method was used to examine several growth variables. Root and shoot length (cm), fresh shoot and root weight, and dry shoot and root weight (g) were measured. The plants were dried in an oven at 70 °C for 48 h to calculate the dry weight.

2.6. Estimation of chlorophyll and carotenoids contents

Lichtenthaler's (1987) method was used for the estimation of photosynthetic pigments. A spectrophotometer was utilized to record the absorbance of the extracted solution at several wavelengths (645, 663, and 470 nm) and a coefficient was used to calculate the chlorophyll contents in *Nigella sativa* leaves.

2.7. Estimation of antioxidant enzyme

Shannon et al. (1966) method was used to analyze Peroxide dismutase. In a 5 mL cuvette, the enzyme was tested by thoroughly combining assay buffer (3.5 mL), diluted enzyme extract (0.1 mL), and o-Dianisidine (0.3 mL). The experiment began with the addition of 0.1 mL of hydrogen peroxide (0.2%) and the simultaneous measurements of the absorbance change at 430 nm was taken. Each sample received its own blank by using boiled enzyme extract. The enzyme's activity was calculated as 0.01 absorbance per minute per mg protein change.

The ability of superoxide dismutase (SOD) to prevent the photochemical reduction of nitro-blue tetrazolium (NBT) was measured using the Beauchamp and Fridovich method (1971). The Nakano and Asada (1981) method was used to measure ascorbate peroxidase (APX). The enzyme activity was determined using the standard equation of absorbance and the molar extinction coefficient of 2.8 mM^{-1} cm^{-1} for ascorbate.

The method of Sinha (1972) for measuring catalase (CAT) activity was somewhat modified. 0.4 mL of 0.2 M hydrogen peroxide, 0.55 mL of 0.1 M potassium phosphate buffer (pH 7.0), and 50 μL of enzyme extract were used in the reaction mixture. It was thoroughly mixed. Incubated for 1 min at room temperature before being treated with a 3.0 mL dichromate reagent. A control reaction was done with 0.4 mL hydrogen peroxide (0.2 M) and 0.6 mL potassium phosphate buffer, but no enzyme extract. For 10 min, the tubes were immersed in boiling water. After cooling, the absorbance at 570 nm was measured with an appropriate blank containing boiling enzyme extract. The sample absorbance was subtracted from the control absorbance.

2.8. Evaluation of hydrogen peroxide and malondialdehyde content

In 5 mL of 0.01 M phosphate buffer (pH 7.0) which was ice-cold, 2 g of tissue were macerated before being centrifuged at 8000 g for 10 min. The collected supernatant was used to calculate the H_2O_2 level (Heath and Packer, 1968).

One gram of tissues was homogenized in 5 mL of TCA (0.1 percent trichloroacetic acid; w/v). Centrifuged for 15 min at 8000×*g*. By the method of Heath and Packer (1968) the supernatant was utilized for MDA estimation. The non-specific absorption values at 600 nm were subtracted, and the MDA concentration was determined at 155 mM^{-1} cm^{-1} using the molar extinction coefficient.

2.9. Estimation of total soluble protein and total soluble sugar

The Bradford test was used to determine the soluble protein concentration (Bradford, 1976). Homogenized 0.5 g of fresh roots and shoots in 10 mL phosphate buffer (pH 7.8) and centrifuged (10,000 rpm) for 20 min. Mixed the protein extraction (0.1 mL) in the solution of 0.9 mL tris-HCl buffer with 5 mL Coomassie reagent (G-250), and stirred well. Allowed it to equilibrate for 2 min at room temperature. Measurement of absorbance was taken at 595 nm with distilled water (blank). The concentrations of protein were calculated using a standard curve of bovine serum albumin (BSA).

The Willis and Yemm (1955) method was used to estimate the soluble sugars, with 0.1 mL of plant extract prepared in 25 mL test tubes. Each tube will be filled with 6 mL of anthrone reagent and to heat up it was placed for 10 min in a boiling bath. The solidification of test tubes was done at room temperature for 10 min. After solidifying they were incubated for 20 min. A spectrophotometer read optical spectrum at 625 nm.

2.10. Statistical analysis

Statistix 8.1 software was used to analyze the data, which provided the mean ± standard error of three replicates. The data were subjected to the one-way ANOVA, the mean test was performed using Tukey's test.

3. Results

3.1. Structural and morphological analysis of nanobiochar sample

The UV–visible spectroscopy is usually the first step to test the sample's purity. The UV–visible absorption spectrum of nBC is shown in Fig. 1(a), exhibiting no absorption bands detected in the visible region (Hosny et al., 2022). Fig. 1(b) shows the XRD pattern of nBC exhibiting the diffraction peaks at 22.5 °, 28.6 °, 37.8 °, 43.1 °, 55.9 °, 65 °, and 73.1 ° with some impurities present in it. A sharp peak at 22.5 ° is showing (002) plane while peak at 28.6 ° making (002) plane is exhibiting the traces of SiO_2. The peak lying at $\theta = 37.8$ ° is showing the traces of CaO making (100) plane. The peak lying at 43.1 ° is exhibiting the traces of $CaCO_3$ making (100) plane. While the minor peaks ***i.e.***, 55.9 °, 65 °, and 73.1 ° shows the traces of SiO_2 and MnO_2 (Dinesh et al., 2018). All peaks correspond to presence of graphitic framework (Siara et al., 2019**)**.

The functional groups of biochar were evaluated through FTIR spectrum, as shown in Fig. 1(c). In the figure, a distinct vibrational peak at about 1018 cm^{-1} is related to C–O bond stretching from carbohydrates. tis may cause the moisture uptake due to hydrophylic nature of carbohydrates based on saturated OH groups, thus resulting in rather sharp peak (Ehsan et al., 2016). The small vibrations in the range 1375–1450 cm^{-1} represent the C–H ($-CH_3$) bending mode. The vibration at 1560 cm^{-1} illustrates aromatic C=C bond. At 1996 cm^{-1}, the vibrations are representing X = C=Y bonding and at 2115 cm^{-1}, the vibrations are showing C ≡ C alkynes bond. Above 2500 to 3000 cm^{-1} vibrations, the traces of C–H (aldehyde) bonds are shown (Pavia et al., 2014). The SEM micrograph of nBC given in Fig. 1(d) shows a porous surface morphology with granular features in the nano regime. These granular features led to the generation of crannies on the surface of the biochar (Adeniyi et al., 2022). These crannies are expected to lead to biochar with large specific surface area (Peterson et al., 2012), which could also affect it a potential catalytic activity and adsorptive capacity (Yu et al., 2011).

3.2. Influence of nanobiochar on plant growth parameters under Cr stress

There was a progressive decrease in the fresh shoot weight (FSW), fresh root weight (FRW), dry shoot weight (DSW), dry root weight (DRW), and root and shoot lengths with the increasing concentration of chromium (Table 1). However, the root length of the plants under chromium stress decreased by 55% and 58% at 200 mg/kg and 300 mg/kg chromium levels, respectively.

A significant increase in the FSW, FRW, DSW and DRW was observed in combination of Cr1 + nBC1 (200 mg/kg + 100mg/L^{-1}) by 176%, 401%, 160% and 400% respectively. In addition, FSW, FRW, DSW and DRW increased by 104%, 13%, 63% and 72% respectively in Cr2 +

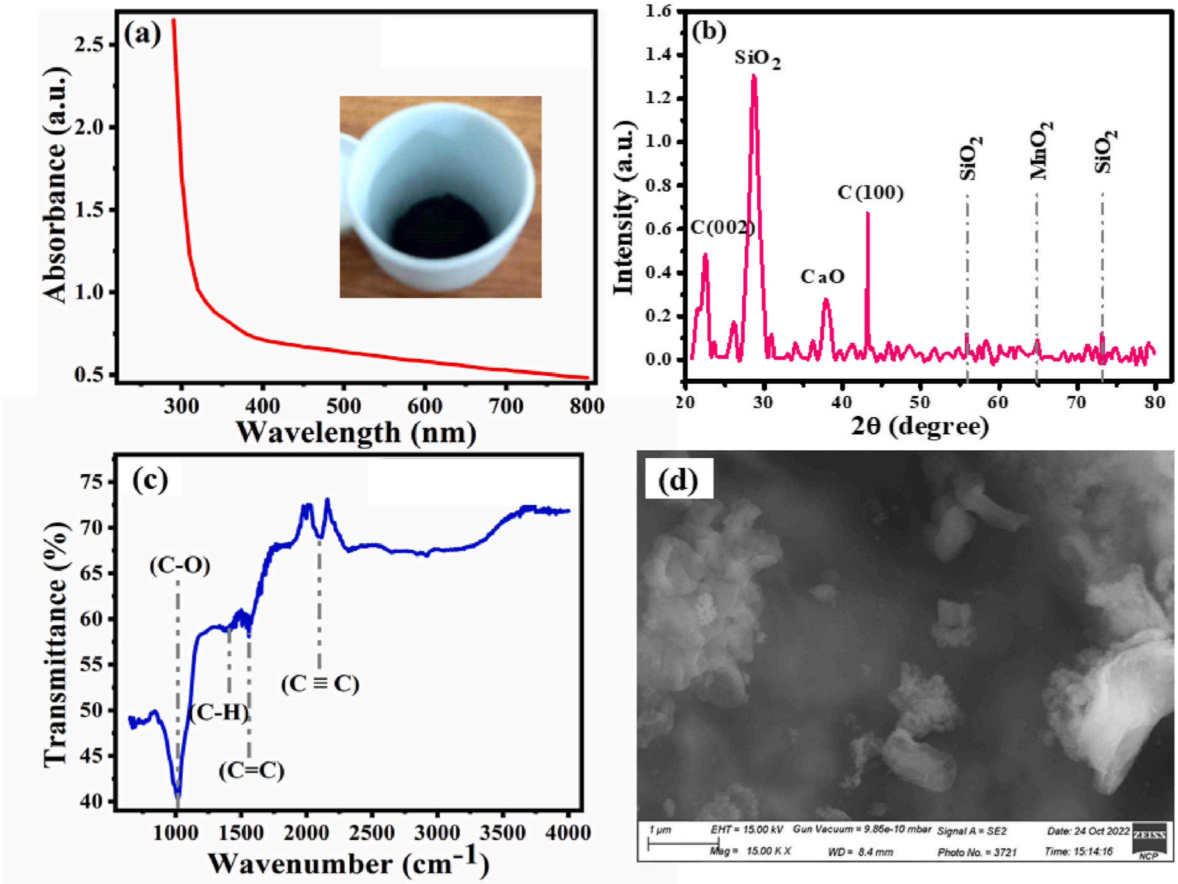

Fig. 1. (a) UV–Vis absorption spectrum of nanobiochar (nBC) with an inset showing the powder form of the sample, (b) XRD pattern of nBC, (c) the corresponding FTIR spectrum showing different functional groups present in the sample and (d) SEM image showing the cranny surface of nBC with granular features.

Table 1
| Effect of nanobiochar on plant growth parameters in *Nigella sativa* under Cr stress.

Treatments	Shoot Length (cm)	Root Length (cm)	FSW (g $plant^{-1}$)	FRW (g $plant^{-1}$)	DSW (g $plant^{-1}$)	DRW (g $plant^{-1}$)
Control	6.36 ± 0.52^{c}	21.5 ± 1.52^{a}	0.07 ± 0.01^{c}	0.01 ± 0.00^{b}	0.01 ± 0.00^{b}	0.00 ± 0.00^{b}
Cr1	8.83 ± 0.88^{ab}	9.5 ± 0.76^{c}	0.15 ± 0.02^{bc}	0.01 ± 0.00^{b}	0.03 ± 0.00^{ab}	0.00 ± 0.00^{b}
Cr2	6.83 ± 0.60^{bc}	8.83 ± 2.12^{c}	0.14 ± 0.03^{bc}	0.01 ± 0.00^{b}	0.05 ± 0.01^{ab}	0.00 ± 0.00^{b}
nBC1	6.3 ± 0.51^{c}	14.5 ± 0.53^{abc}	0.06 ± 0.00^{c}	0.01 ± 0^{b}	0.01 ± 0^{c}	0.00 ± 0.00^{b}
Cr1+nBC1	9.9 ± 0.1^{a}	20.83 ± 1.01^{ab}	0.43 ± 0.08^{a}	0.06 ± 0.00^{a}	0.08 ± 0.00^{a}	0.04 ± 0.00^{a}
Cr2+nBC1	6.33 ± 0.33^{c}	11.7 ± 4.39^{bc}	0.09 ± 0.04^{bc}	0.02 ± 0.01^{b}	0.02 ± 0.01^{c}	0.01 ± 0.00^{b}
nBC2	5.73 ± 0.43^{c}	14.8 ± 1.20^{abc}	0.08 ± 0.00^{c}	0.01 ± 0.00^{b}	0.01 ± 0^{c}	0.00 ± 0.00^{b}
Cr1+nBC2	7.66 ± 0.33^{abc}	8 ± 0.28^{c}	0.09 ± 0.00^{bc}	0.01 ± 0.00^{b}	0.02 ± 0^{c}	0.00 ± 0.00^{b}
Cr2+nBC2	9.83 ± 0.16^{a}	14.6 ± 1.87^{abc}	0.29 ± 0.06^{ab}	0.02 ± 0.00^{b}	0.05 ± 0.01^{ab}	0.01 ± 0.00^{b}

Different statistical groups are represented by different letters suggested by the Tukey-HSD pair-wise multiple comparison at $p < 0.05$. Cr1 = 200 mg/kg Cr stress, Cr2 = 300 mg/kg Cr stress, nBC1 = 100 mg/L nanobiochar, nBC2 = 150 mg/L nanobiochar, Cr1+nBC1 = 200 mg/kg + 100 mg/L, Cr1+nBC2 = 200 mg/kg + 150 mg/L, Cr2+nBC1 = 300 mg/kg + 100 mg/L, Cr2+nBC2 = 300 mg/kg + 150 mg/L. FSW = Fresh shoot weight, FRW = Fresh root weight, DSW = Dry shoot weight, DRW = Dry root weight.

nBC2 (300 mg/kg + 150 mg/L). An increase of 12% in the shoot length was observed in the plants with combination of Cr1 + nBC1 (200 mg/kg + 100 mg/L) as compared to sole treatment of Cr1 (200 mg/kg) (Table 1). However, shoot length of the plant decreased in Cr1 + nBC2 (200 mg/kg + 150 mg/L) by 13% and increased in Cr2 + nBC2 (300 mg/kg + 150 mg/L) by 43% respectively. A significant increase in plant root length was observed in both treatments i.e. Cr1 + nBC1 & Cr2 + nBC2 by 119% and 66% respectively.

3.2.1. *Nanobiochar improves photosynthetic pigments in Nigella sativa under Cr stress*

When subjected to stress, plants respond mainly through alteration in the physiological process. The application of nBC probably mitigated the chlorophyll damage of chromium to *Nigella sativa* as reflected by the changes in chlorophyll contents. It was noted that 300 mg/kg Cr in soil could greatly decline the chlorophyll *a, b,* and carotenoid contents of *Nigella sativa* seedlings by 12%, 24%, and 44% respectively relative to Cr-free control (Fig. 2). The increased chlorophyll *a, and b* contents were observed in Cr2 + nBC1 (300 mg/kg + 100 mg/L) by 69% and 79%. However, under Cr2 + nBC2 (300 mg/kg + 150 mg/L) treatment by 79% and 91% respectively as compared to control. The increased carotenoid content was observed in Cr1 + nBC1 (200 mg/kg + 100 mg/L) by 5% relative to sole treatment of Cr1 (200 mg/kg) (Fig. 2).

3.2.2. *Nanobiochar mitigates Cr-induced oxidative stress in Nigella sativa*

The oxidative stress was measured in terms of hydrogen peroxide (H_2O_2) and malondialdehyde acetate (MDA) content. MDA and H_2O_2 were increased in shoots by 35% and 46% and in roots by 18% and 48% respectively, under Cr2 (300 mg/kg) as compared to control (Fig. 3). However, decrease in the MDA and H2O2 content was observed in

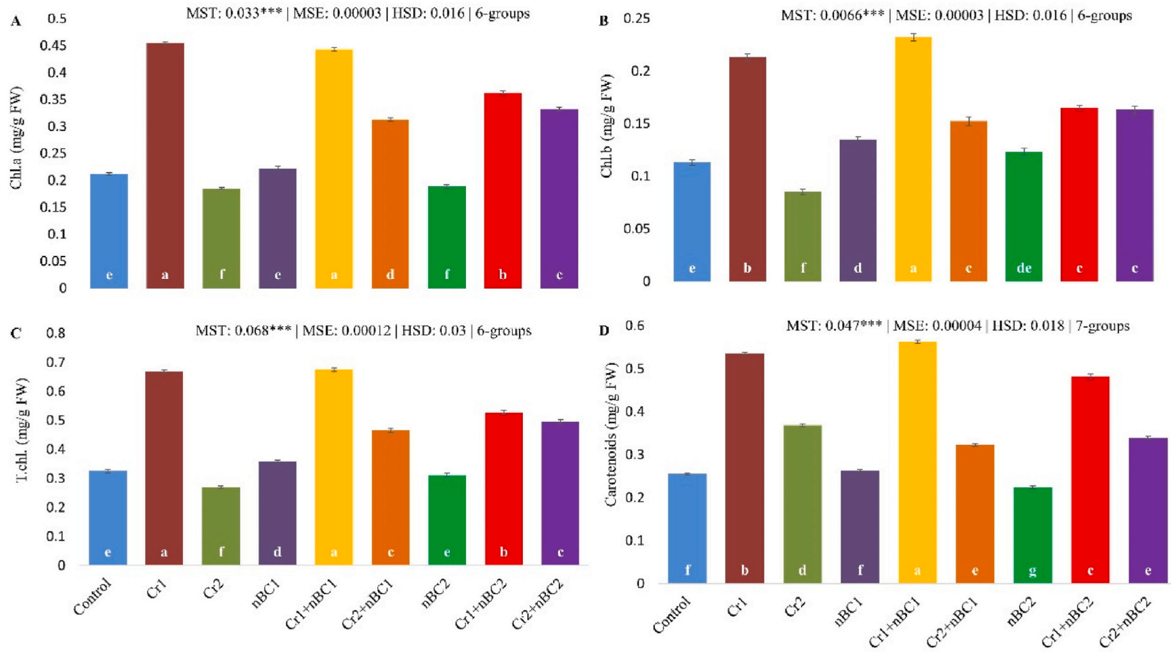

Fig. 2. | Effect of nanobiochar on physiological parameters (Chlorophyll 'a' A, Chlorophyll 'b' B, Total chlorophyll C and carotenoids D) under chromium stress in *Nigella sativa.* The data represents the means ± SE ($P \leq 0.05$). Different statistical groups are represented by different letters suggested by the Tukey-HSD pair-wise multiple comparison at $p < 0.05$. In figures * = significant at 0.05, ** = significant at 0.01, and *** = significant at 0.001 levels. Mean square of treatment (MST) and error (MSE) are given along with honest significant difference (HSD) value and number of groups obtained after comparison.
Cr1 = 200 mg/kg Cr stress, Cr2 = 300 mg/kg Cr stress, nBC1 = 100 mg/L nanobiochar, nBC2 = 150 mg/L nanobiochar, Cr1+nBC1 = 200 mg/kg + 100 mg/L, Cr1+nBC2 = 200 mg/kg + 150 mg/L, Cr2+nBC1 = 300 mg/kg + 100 mg/L, Cr2+nBC2 = 300 mg/kg + 150 mg/L.

shoots with combination of Cr2 + nBC1 (300 mg/kg + 100 mg/L) by 14% and 21% and in Cr2 + nBC2 (300 mg/kg + 150 mg/L) by 15% and 1% respectively.

Furthermore, it was observed that the MDA content in roots decreased with the increasing concentration of chromium in the combination of Cr1 + nBC2 and Cr2 + nBC2 by 24% and 19% respectively as compared to sole stress of Cr1 (200 mg/kg) and Cr2 (300 mg/kg) respectively. Besides, H2O2 decreased by 16% and 30% in roots under Cr2 + nBC1 (300 mg/kg + 100 mg/L) and Cr2 + nBC2 (300 mg/kg + 150 mg/L) treatments respectively.

3.2.3. *Nanobiochar induced osmoprotectant contents in Nigella sativa under Cr stress*

To determine the ameliorative effect of nBC against chromium in *Nigella sativa,* total soluble protein and total soluble sugar were also analyzed. The total soluble protein and sugar in Cr1 (200 mg/kg) treated plants were declined than the Cr2 (300 mg/kg) treated seedlings as shown in Fig. 4. An increased level of total soluble sugar was observed after sole application of nBC1 (100 mg/L) and nBC2 (150 mg/L) in shoots by 6% and 18% and in roots by 1% and 19% respectively relative to control. However, the increase in total soluble sugar was observed in the combination of Cr1 + nBC2 (200 mg/kg + 150 mg/L) in shoots by 26% and roots by 37%.

However, the minimum increased total soluble protein was observed in shoots with the combination of Cr1 + nBC1 (200 mg/kg + 100 mg/L) by 3%. Besides, the increased total soluble protein of roots was observed in the combination of Cr2 + nBC1 (300 mg/kg + 100 mg/L) by 2%.

3.2.4. *Nanobiochar regulates antioxidant enzymes in Nigella sativa under Cr stress*

An enzymatic antioxidant system including Catalase (CAT), Superoxide dismutase (SOD), peroxidase dismutase (POD), and ascorbic peroxidase (APX) played a crucial role in scavenging harmful oxygen species. The impact of nBC on antioxidant enzyme activities in *Nigella sativa* leaves and roots under chromium stress is presented in Fig. 5.

The activities of CAT, SOD, POD, and APX under Cr1 (200 mg/kg) stress were declined than the Cr2 (300 mg/kg) treated seedlings. The increased activity of CAT (8% and 11%), SOD (3% and 14%), POD (2% and 10%) and APX (10% and 27%) was observed in shoots after sole application of nBC1 (100 mg/L) and nBC2 (150 mg/L) respectively relative to control. In addition, in roots, activity of CAT (8% and 3%) and SOD (8% and 13%) was increased after application of nBC1 (100 mg/L) and nBC2 (150 mg/L) respectively, compared to control. Besides, the increased CAT, SOD, POD and APX activity was observed in shoots of the seedlings in Cr1 + nBC2 (200 mg/kg + 150 mg/L) by 5%, 24%, 13%and 17% respectively. The CAT level was increased in roots with combination of Cr1 + nBC2 (200 mg/kg + 150 mg/L) and Cr2 + nBC2 (300 mg/kg + 150 mg/L) by 4.9% and 4.4% as compared to Cr1 and Cr2 (200 mg/kg and 300 mg/kg) alone. The activity of SOD increased in roots with combination of Cr1 + nBC1 (200 mg/kg + 100 mg/L) and Cr1 + nBC2 (200 mg/kg + 150 mg/L) by 18% and 9% respectively, (Fig. 5).

The POD level in roots decreased with the increasing concentration of chromium in Cr1 + nBC1 (200 mg/kg + 100 mg/L) and Cr2 + nBC1 (300 mg/kg + nBC1) by 6% and 4% respectively. An increase in POD level was observed after application of nBC2 in combination of Cr1 + nBC2 (200 mg/kg + 150 mg/L) by 6%. However, an increase in activity of APX was observed after application of Cr1 + nBC2 (200 mg/kg + 150 mg/L) by 11%.

4. Discussion

Globally, chromium toxicity in cultivable areas has become a significant issue (Vivas et al., 2006). In the current study, *Nigella sativa* growth reduced as chromium concentration increased. Many authors reported similar findings, stating that Cr preferentially tends to accumulate in roots of plants and that stress of Cr has negative effects on growth of root (Gupta et al., 2018). Length of roots in *Cicer arietinum* and *Allium cepa* L. decreased with the increase in concentration of Cr (Medda and Mondal, 2017; Gupta et al., 2018). Stress of Cr in higher concentrations not only harm the roots but also have negative effects on the

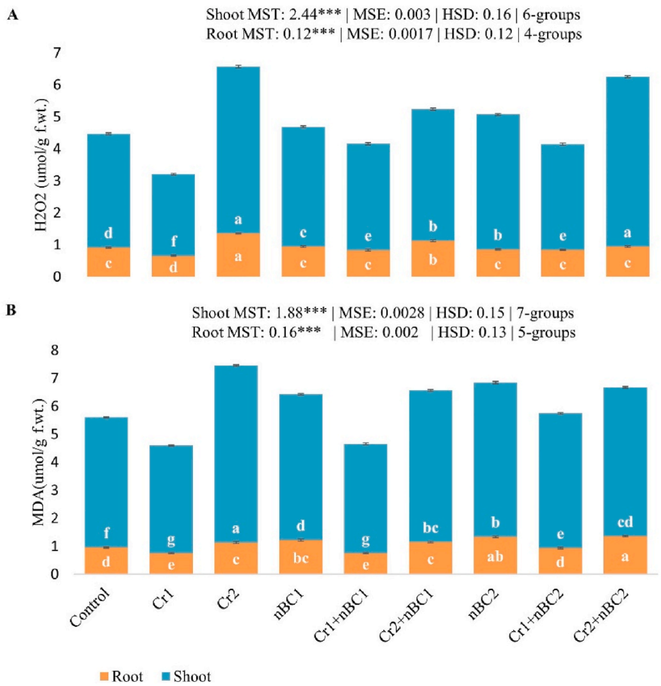

Fig. 3. | Effect of nanobiochar on plant oxidative stress (Hydrogen peroxide (H2O2) content A, and Malondialdehyde acetate (MDA) content B) under chromium stress in *Nigella sativa.* The data represents the means ± SE (n = 5). Different statistical groups are represented by different letters suggested by the Tukey-HSD pair-wise multiple comparisons at $p < 0.05$. In figures * = significant at 0.05, ** = significant at 0.01, and *** = significant at 0.001 levels. Mean square of treatment (MST) and error (MSE) are given along with the honest significant difference (HSD) value and the number of groups obtained after comparison.
Cr1 = 200 mg/kg Cr stress, Cr2 = 300 mg/kg Cr stress, nBC1 = 100 mg/L nanobiochar, nBC2 = 150 mg/L nanobiochar, Cr1+nBC1 = 200 mg/kg + 100 mg/L, Cr1+nBC2 = 200 mg/kg + 150 mg/L, Cr2+nBC1 = 300 mg/kg + 100 mg/L, Cr2+nBC2 = 300 mg/kg + 150 mg/L.

shoots (Table 1). Cr in the growth medium affected stem development and the dry weight of many plants such as *Cicer arietinum* L., *Phaseolus aureus* L., and *Amaranthus viridis* L. (Singh and Sharma, 2017; Liu et al., 2008). The main cause of the reduction in plant length and growth of stem could be that the stress of Cr slow down the growth of roots, which reduces the transport of water and vital nutrients to the plant's aerial parts (Kapoor et al., 2022; Rai et al., 2007). This study measured the impact of foliar sprays of nBC on reducing Cr toxicity in *Nigella sativa* seedlings and analyzed Morpho-physiological parameters. According to the findings of the present study, foliar spray of nBC dramatically increased seedling growth and prevented the detrimental effects of Cr on *Nigella sativa* seedlings **(Table 1).** The current study's findings are comparable with prior studies in which banana peel and tea waste-derived biochar improved wheat shoot and root biomass (Sial et al., 2019), wheat with rice straw biochar (Ali et al., 2020), and lettuce biomass with pistachio shell biochar (Turan et al., 2018). The increase in biomass and growth of *Nigella sativa* plants are consistent with earlier research findings of an increase in biomass of Cassia alata L. (Huang et al., 2018) and eggplant (Edenborn et al., 2018; Mohan et al., 2018) due to the application of biochar in heavy metals treated soil was recorded. The mechanism responsible for this increase in *Nigella sativa* biomass could be related to nBC integration with the plant, which gives vital nutrients to the plants (Zheng et al., 2018; Faria et al., 2018).

Our findings showed that the chlorophyll content of *Nigella sativa* reduced as the chromium concentration increased. In consistence to our findings, Chlorophyll concentration decreases induced by stress of chromium have also been recorded in a variety of plants, including *Glycine* max L, *Hibiscus esculentus* L., *Cicer arietinum,* and *Taxiphyllum taxirameum* (Basit et al., 2022; Amin et al., 2013; Medda and Mondal, 2017; Chen et al., 2018). In our investigation, the presence of nBC reduced the physiological damage caused by Cr to *Nigella sativa* plants, as measured by chlorophyll changes (Fig. 2). Similar to our findings, Cd in aqueous solutions was found to significantly reduce the chlorophyll content of rice seedlings (Guo et al., 2018). The high Pb levels in the soil affected wheat photosynthesis (Hasanuzzaman et al., 2018). However, according to our findings chlorophyll *a and b*, as well as total chlorophyll contents, were significantly increased by nBC addition. Partial incorporation of biochar into a Ni-rich soil increased photosynthetic activity in *Trifolium pretense* L., which is consistent with our findings (Shahbaz et al., 2018a). With a few exceptions, we observed that all treatments significantly increased the total soluble sugar and total soluble protein content in *Nigella sativa* plants over data from the corresponding control (Fig. 4). These findings align with the beneficial function of biochar in the increase of protein content in both maize and sunflower (Shahbaz et al., 2018b) exposed to heavy metal stress.

In our investigation, we observed that Cr increased ROS formation, such as H_2O_2 and hydroxyl compounds, which elevates MDA levels. The activity of antioxidative enzyme systems in plants increased under Cr stress in order to scavenge the excess ROS generated and offset their negative effects (Srivastava et al., 2021). In the current study, increasing amounts of Cr treatment boosted antioxidant enzyme activity. Similar to our findings, after being exposed to Cr(VI) (20 mg/L), *Calotropis procera* showed an increase in SOD and CAT activity, with activities of SOD becoming the maximum (Usman et al., 2020). The synthesis of reducing agents (AsA and GSH metabolites), which catalyzes the reduction of H_2O_2 to O_2 and H_2O, is aided by the synergistic effects of APX and CAT, which both play critical roles in scavenging of ROS (Bhaduri and Fulekar, 2012; Bashir et al., 2020). In this study, we observed that using nBC reduced the levels of reactive oxygen species (H_2O_2 and MDA) (Fig. 3) in *Nigella sativa* shoot and roots but also increased antioxidant enzyme production (SOD, CAT, and APX) (Fig. 5). It has been reported that reactive oxygen species can be produced during charring and retained in biochar particles for hours or days (Lomnicki et al., 2008), as well as months (Liao et al., 2014). According to the present study, the addition of nBC increased these antioxidant enzymes in *Nigella sativa* seedlings when compared to the control (Fig. 5). These findings can be align with the findings of Turan et al. (2018) and Ramzani et al. (2017) where biochar treatment to heavy metal contaminated soils improved CAT, APX, and SOD activities in sunflower and mung bean.

5. Conclusion

The toxicity of chromium (200 mg/kg and 300 mg/kg) in *Nigella sativa* seedlings was increased oxidative stress. The toxic effects of chromium (Cr) increased with the increase in chromium concentration. This study revealed that foliar application of nanobiochar (nBC) provided an effective method to alleviate the toxic effect of Cr on *Nigella sativa* seedlings, which could improve the growth, photosynthesis, osmoprotectants, and antioxidant enzyme system in *Nigella sativa* seedlings under Cr stress. The nBC treatment of 100 mg/L showed better results than 150 mg/L in the mitigation of Cr stress (200 mg/kg). The results clearly showed that with a high concentration of chromium (300 mg/kg) the application of nBC (100 mg/L) significantly reduced hydrogen peroxide (H_2O_2) and malondialdehyde acetate (MDA) levels in the roots and shoots of *Nigella sativa* seedlings. However, seedlings treated with 150 mg/L nBC enhanced the activity of antioxidant enzymes (Catalase (CAT), Superoxide dismutase (SOD), peroxide dismutase (POD), and ascorbic peroxidase (APX)) as compared to 100 mg/L under Cr stress (200 mg/nBC). Thus, 100 mg/L of nBC was the most effective treatment for the mitigation of Cr stress in *Nigella sativa* seedlings. It is recommended that further field investigations are necessary to test it in terms of practicality and cost-effectiveness at the field scale.

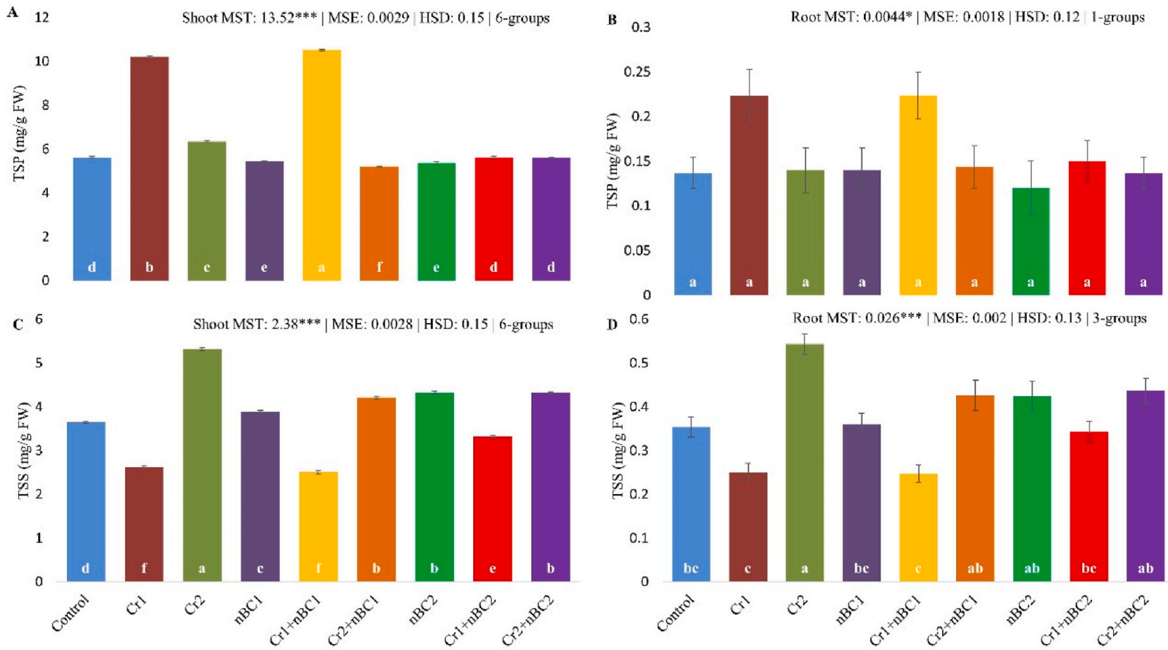

Fig. 4. | Effect of nanobiochar on plant osmoprotectants (Total soluble protein (TSP) in shoots A, Total soluble protein (TSP) in roots B, Total soluble sugar (TSS) in shoots C, and Total soluble sugar (TSS) in roots D) under chromium stress in *Nigella sativa.* The data represents the means ± SE (n = 5). Different statistical groups are represented by different letters suggested by the Tukey-HSD pair-wise multiple comparisons at $p < 0.05$. In figures * = significant at 0.05, ** = significant at 0.01, and *** = significant at 0.001 levels. Mean square of treatment (MST) and error (MSE) are given along with the honest significant difference (HSD) value and the number of groups obtained after comparison.
Cr1 = 200 mg/kg Cr stress, Cr2 = 300 mg/kg Cr stress, nBC1 = 100 mg/L nanobiochar, nBC2 = 150 mg/L nanobiochar, Cr1+nBC1 = 200 mg/kg + 100 mg/L, Cr1+nBC2 = 200 mg/kg + 150 mg/L, Cr2+nBC1 = 300 mg/kg + 100 mg/L, Cr2+nBC2 = 300 mg/kg + 150 mg/L.

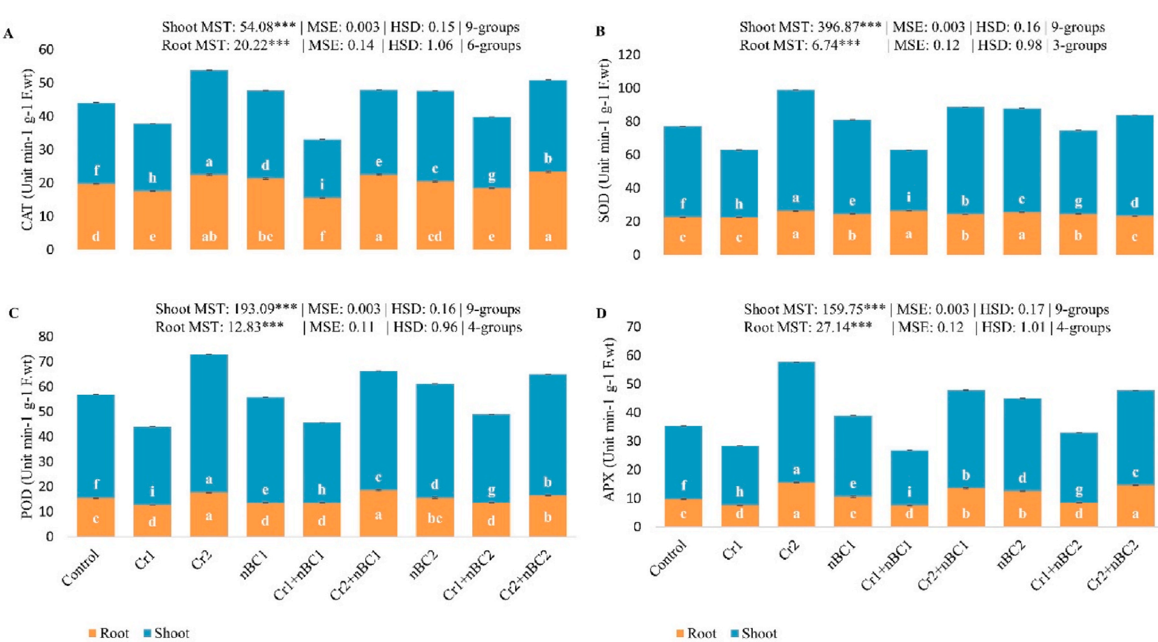

Fig. 5. | Effect of nanobiochar on plant antioxidant enzymes (Catalase enzyme (CAT) A), Superoxide dismutase (SOD) activity B, Peroxidase dismutase (POD) C, and Ascorbate peroxidase (APX) activity D) under chromium stress in *Nigella sativa.* The data represents the means ± SE (n = 5). Different statistical groups are represented by different letters suggested by the Tukey-HSD pair-wise multiple comparisons at $p < 0.05$. In figures * = significant at 0.05, ** = significant at 0.01, and *** = significant at 0.001 levels. Mean square of treatment (MST) and error (MSE) are given along with the honest significant difference (HSD) value and the number of groups obtained after comparison.
Cr1 = 200 mg/kg Cr stress, Cr2 = 300 mg/kg Cr stress, nBC1 = 100 mg/L nanobiochar, nBC2 = 150 mg/L nanobiochar, Cr1+nBC1 = 200 mg/kg + 100 mg/L, Cr1+nBC2 = 200 mg/kg + 150 mg/L, Cr2+nBC1 = 300 mg/kg + 100 mg/L, Cr2+nBC2 = 300 mg/kg + 150 mg/L.

Contribution

Dr. Musarrat and Dr. Shahid conceived, planned and supervised the green house and lab experiments respectively, and wrote this manuscript. Arooj Zia carried out greenhouse experiments. Arooj Zia and Hina Ashraf analyzed physio-biochemical parameters. Dr. Anis Ali Shah interpreting the results and worked on manuscript. Ghulam Farid provide technical support and has done all computational work and construct graphs. All authors discussed the results and commented on the manuscript.

Declaration of competing interest

The authors declare that they have no known competing financial interests or personal relationships that could have appeared to influence the work reported in this paper.

Data availability

Data will be made available on request.

References

Abbas, A., Azeem, M., Naveed, M., Latif, A., Bashir, S., Ali, A., Ali, L., 2020. Synergistic use of biochar and acidified manure for improving growth of maize in chromium contaminated soil. Int. J. Phytoremediation 22 (1), 52–61.

Adeniyi, A.G., Abdulkareem, S.A., Iwuozor, K.O., Ogunniyi, S., Abdulkareem, M.T., Emenike, E.C., Sagboye, P.A., 2022. Effect of salt impregnation on the properties of orange albedo biochar. Cleaner Chem. Eng. 3, 100059.

Ahmad, I., Tripathi, J., Manik, S., Umar, L., Rabia, J., 2013. Preliminary phytochemical studies of the miracle herb of the century, *Nigella sativa* L. (Black Seed). Indo American Journal of Pharmaceutical Research 3 (4), 3000–3007.

AkilaKesavan, G., 2014. Nanotechnology and its applications. SciTech J. 1 (6), 12–13.

Al-Bukhari, S. Sahih Al-Bukhari 5687 Book 76 Hadith 10.

Ali, S.A., Parveen, N., Ali, A.S., 2018. Links between the Prophet Muhammad (PBUH) recommended foods and disease management: a review in the light of modern superfoods. Int. J. Health Sci. 12 (2), 61.

Ali, U., Shaaban, M., Bashir, S., Gao, R., Fu, Q., Zhu, J., Hu, H., 2020. Rice straw, biochar and calcite incorporation enhance nickel (Ni) immobilization in contaminated soil and Ni removal capacity. Chemosphere 244, 125418.

Alimohammadi, M., Xu, Y., Wang, D., Biris, A.S., Khodakovskaya, M.V., 2011. Physiological responses induced in tomato plants by a two-component nanostructural system composed of carbon nanotubes conjugated with quantum dots and its in vivo multimodal detection. Nanotechnology 22 (29), 295101.

Allah Ditta, H.M., Aziz, A., Hussain, M.K., Mehboob, N., Hussain, M., Farooq, S., Azhar, M.F., 2021. Exogenous application of black cumin (*Nigella sativa*) seed extract improves maize growth under chromium (Cr) stress. Int. J. Phytoremediation 23 (12), 1231–1243.

Amin, H., Arain, B.A., Amin, F., Surhio, M.A., 2013. Phytotoxicity of Chromium on Germination, Growth and Biochemical Attributes of *Hibiscus Esculentus* L. American Journal of Plant Sciences, 2013.

Ashfaq, M., Verma, N., Khan, S., 2017. Carbon nanofibers as a micronutrient carrier in plants: efficient translocation and controlled release of Cu nanoparticles. Environ. Sci. J. Integr. Environ. Res.: Nano 4 (1), 138–148.

Badary, O.A., Taha, R.A., Gamal El-Din, A.M., Abdel-Wahab, M.H., 2003. Thymoquinone is a potent superoxide anion scavenger. Drug Chem. Toxicol. 26 (2), 87–98.

Bashir, M.A., Naveed, M., Ahmad, Z., Gao, B., Mustafa, A., Núñez-Delgado, A., 2020. Combined application of biochar and sulfur regulated growth, physiological, antioxidant responses and Cr removal capacity of maize (*Zea mays* L.) in tannery polluted soils. Journal of environmental management 259, 110051.

Basit, F., Bhat, J.A., Guan, Y., Jan, B.L., Tyagi, A., Ahmad, P., 2022. Nitric oxide and spermine revealed positive defense interplay for the regulation of the chromium toxicity in soybean (Glycine max L.). Environ. Pollut. 308, 119602.

Beauchamp, C., Fridovich, I., 1971. Superoxide dismutase: improved assays and an assay applicable to acrylamide gels. Anal. Biochem. 44 (1), 276–287.

Bhaduri, A.M., Fulekar, M.H., 2012. Antioxidant enzyme responses of plants to heavy metal stress. Rev. Environ. Sci. Biotechnol. 11 (1), 55–69.

Bradford, M.M., 1976. A rapid and sensitive method for the quantitation of microgram quantities of protein utilizing the principle of protein-dye binding. Anal. Biochem. 72 (1–2), 248–254.

Chen, Y.E., Mao, H.T., Ma, J., Wu, N., Zhang, C.M., Su, Y.Q., Yuan, S., 2018. Biomonitoring chromium III or VI soluble pollution by moss chlorophyll fluorescence. Chemosphere 194, 220–228.

Christou, A., Georgiadou, E.C., Zissimos, A.M., Christoforou, I.C., Christofi, C., Neocleous, D., Fotopoulos, V., 2021. Uptake of hexavalent chromium by *Lactuca sativa* and *Triticum aestivum* plants and mediated effects on their performance, linked with associated public health risks. Chemosphere 267, 128912.

Coetzee, J.J., Bansal, N., Chirwa, E., 2020. Chromium in environment, its toxic effect from chromite-mining and ferrochrome industries, and its possible bioremediation. Exposure and health 12 (1), 51–62.

Danish, S., Kiran, S., Fahad, S., Ahmad, N., Ali, M.A., Tahir, F.A., Nasim, W., 2019a. Alleviation of chromium toxicity in maize by Fe fortification and chromium tolerant ACC deaminase producing plant growth promoting rhizobacteria. Ecotoxicol. Environ. Saf. 185, 109706.

Danish, S., Tahir, F.A., Rasheed, M.K., Ahmad, N., Ali, M.A., Kiran, S., Butt, B., 2019b. Effect of foliar application of Fe and banana peel waste biochar on growth, chlorophyll content and accessory pigments synthesis in spinach under chromium (IV) toxicity. Open Agriculture 4 (1), 381–390.

Dazy, M., Béraud, E., Cotelle, S., Meux, E., Masfaraud, J.F., Férard, J.F., 2008. Antioxidant enzyme activities as affected by trivalent and hexavalent chromium species in *Fontinalis antipyretica* Hedw. Chemosphere 73 (3), 281–290.

Dinesh, M., Kumar, A., Ankur, S., Manvendra, P., Prachi, S., Charles, U., Pittman, J., 2018. Biochar production and applications in soil fertility and carbon sequestration – a sustainable solution to crop-residue burning in India. RSC Adv. 8 (5), 508–520.

Edenborn, S.L., Johnson, L.M., Edenborn, H.M., Albarran-Jack, M.R., Demetrion, L.D., 2018. Amendment of a hardwood biochar with compost tea: effects on plant growth, insect damage and the functional diversity of soil microbial communities. Biol. Agric. Hortic. 34 (2), 88–106.

EFSA Panel on Contaminants in the Food Chain (CONTAM), 2015. Scientific Opinion on the risks to public health related to the presence of nickel in food and drinking water. EFSA J. 13 (2), 4002.

Ehsan, N., Nawaz, R., Ahmad, S., Khan, M.M., Hayat, J., 2016. Phytoremediation of chromium contaminated soil by an ornamental plant Vinca (Vinca rosea L.). J. Environ. 7, 29–34.

El-Dakhakhny, M., Madi, N.J., Lembert, N., Ammon, H.P.T., 2002. *Nigella sativa* oil, nigellone and derived thymoquinone inhibit synthesis of 5-lipoxygenase products in polymorphonuclear leukocytes from rats. J. Ethnopharmacol. 81 (2), 161–164.

Faria, W.M., Figueiredo, C.C.D., Coser, T.R., Vale, A.T., Schneider, B.G., 2018. Is sewage sludge biochar capable of replacing inorganic fertilizers for corn production? Evidence from a two-year field experiment. Arch. Agron Soil Sci. 64 (4), 505–519.

Gill, S.S., Hasanuzzaman, M., Nahar, K., Macovei, A., Tuteja, N., 2013. Importance of nitric oxide in cadmium stress tolerance in crop plants. Plant Physiol. Biochem. 63, 254–261.

Guo, L., Chen, A., He, N., Yang, D., Liu, M., 2018. Exogenous silicon alleviates cadmium toxicity in rice seedlings in relation to Cd distribution and ultrastructure changes. J. Soils Sediments 18 (4), 1691–1700.

Gupta, K., Mishra, K., Srivastava, S., Kumar, A., 2018. Cytotoxic assessment of chromium and arsenic using chromosomal behavior of root meristem in *Allium cepa* L. Bull. Environ. Contam. Toxicol. 100 (6), 803–808.

Hafiz, M.F., Ma, L., 2021. Effect of chromium on seed germination, early seedling growth and chromium accumulation in tomato genotypes. Acta Physiol. Plant. 43 (7), 1–11.

Hasanuzzaman, M., Nahar, K., Rahman, A., Mahmud, J.A., Alharby, H.F., Fujita, M., 2018. Exogenous glutathione attenuates lead-induced oxidative stress in wheat by improving antioxidant defense and physiological mechanisms. J. Plant Interact. 13 (1), 203–212.

Heath, R.L., Packer, L., 1968. Photoperoxidation in isolated chloroplasts: I. Kinetics and stoichiometry of fatty acid peroxidation. Arch. Biochem. Biophys. 125 (1), 189–198.

Hosseini, M., Zakeri, S., Khoshdast, S., Yousefian, F.T., Rastegar, M., Vafaee, F., Kazemi, S.A., 2012. The effects of *Nigella sativa* hydro-alcoholic extract and thymoquinone on lipopolysaccharide-induced depression like behavior in rats. J. Pharm. BioAllied Sci. 4 (3), 219.

Hosny, M., Fawzy, M., Eltaweil, A.S., 2022. Green synthesis of bimetallic Ag/ZnO@ Biohar nanocomposite for photocatalytic degradation of tetracycline, antibacterial and antioxidant activities. Sci. Rep. 12, 7316. https://doi.org/10.1038/s41598-022-11014-0.

Huang, L., Li, Y., Zhao, M., Chao, Y., Qiu, R., Yang, Y., Wang, S., 2018. Potential of *Cassia alata* L. coupled with biochar for heavy metal stabilization in multi-metal mine tailings. Int. J. Environ. Res. Publ. Health 15 (3), 494.

Islam, F., Yasmeen, T., Arif, M.S., Riaz, M., Shahzad, S.M., Imran, Q., Ali, I., 2016. Combined ability of chromium (Cr) tolerant plant growth promoting bacteria (PGPB) and salicylic acid (SA) in attenuation of chromium stress in maize plants. Plant Physiol. Biochem. 108, 456–467.

Jaishankar, M., Tseten, T., Anbalagan, N., Mathew, B.B., Beeregowda, K.N., 2014. Toxicity, mechanism and health effects of some heavy metals. Interdiscipl. Toxicol. 7 (2), 60.

Jan, S., Noman, A., Kaya, C., Ashraf, M., Alyemeni, M.N., Ahmad, P., 2020. 24-Epibrassinolide alleviates the injurious effects of Cr (VI) toxicity in tomato plants: insights into growth, physio-biochemical attributes, antioxidant activity and regulation of Ascorbate–glutathione and Glyoxalase cycles. J. Plant Growth Regul. 39 (4), 1587–1604.

Javed, M.T., Tanwir, K., Abbas, S., Saleem, M.H., Iqbal, R., Chaudhary, H.J., 2021. Chromium retention potential of two contrasting *Solanum lycopersicum* Mill. cultivars as deciphered by altered pH dynamics, growth, and organic acid exudation under Cr stress. Environ. Sci. Pollut. Control Ser. 28 (22), 27542–27554.

Kanter, M., Coskun, O., Gurel, A., 2005. Effect of black cumin (*Nigella sativa*) on cadmium-induced oxidative stress in the blood of rats. Biol. Trace Elem. Res. 107 (3), 277–287.

Kapoor, R.T., Mfarrej, M.F.B., Alam, P., Rinklebe, J., Ahmad, P., 2022. Accumulation of Chromium in Plants and its Repercussion in Animals and Humans. Environmental Pollution, 119044.

Khattak, A., Ullah, F., Shinwari, Z.K., Mehmood, S., 2021. The effect of titanium dioxide nanoparticles and salicylic acid on growth and biodiesel production potential of

sunflower (*Helianthus annuus* L.) under water stress. Pakistan J. Bot. 53 (6), 1987–1995.
Khodakovskaya, M.V., Kim, B.S., Kim, J.N., Alimohammadi, M., Dervishi, E., Mustafa, T., Cernigla, C.E., 2013. Carbon nanotubes as plant growth regulators: effects on tomato growth, reproductive system, and soil microbial community. Small 9 (1), 115–123.
Kishwar, F., Anwar, H., 2012. Use of active ingredient of *Nigella sativa* to reduce toxicity of some trace elements (Fe (III), Cr (VI), Cu (II), V (IV) and Co (II)). FUUAST Journal of Biology 2 (2 December), 95–101.
Kishwar, F., Mahmood, T., Mahmood, I., 2016. Complexation of active ingredient thymoquinone of *Nigella sativa* (black seed) with chromium (VI). FUUAST Journal of Biology 6 (1), 65–72.
Lehmann, J., Kuzyakov, Y., Pan, G., Ok, Y.S., 2015. Biochars and the plant-soil interface. Plant Soil 395, 1–5.
Liao, S., Pan, B., Li, H., Zhang, D., Xing, B., 2014. Detecting free radicals in biochars and determining their ability to inhibit the germination and growth of corn, wheat and rice seedlings. Environ. Sci. Technol. 48 (15), 8581–8587.
Lichtenthaler, H.K., 1987. [34] Chlorophylls and carotenoids: pigments of photosynthetic biomembranes. In: Methods in Enzymology, vol. 148. Academic Press, pp. 350–382.
Liu, D., Zou, J., Wang, M., Jiang, W., 2008. Hexavalent chromium uptake and its effects on mineral uptake, antioxidant defence system and photosynthesis in *Amaranthus viridis* L. Bioresour. Technol. 99 (7), 2628–2636.
Liu, W., Li, Y., Feng, Y., Qiao, J., Zhao, H., Xie, J., Liang, S., 2020. The effectiveness of nanobiochar for reducing phytotoxicity and improving soil remediation in cadmium-contaminated soil. Sci. Rep. 10 (1), 1–10.
Lomnicki, S., Truong, H., Vejerano, E., Dellinger, B., 2008. Copper oxide-based model of persistent free radical formation on combustion-derived particulate matter. Environ. Sci. Technol. 42 (13), 4982–4988.
Medda, S., Mondal, N.K., 2017. Chromium toxicity and ultrastructural deformation of *Cicer arietinum* with special reference of root elongation and coleoptile growth. Annals of Agrarian Science 15 (3), 396–401.
Mohan, D., Abhishek, K., Sarswat, A., Patel, M., Singh, P., Pittman, C.U., 2018. Biochar production and applications in soil fertility and carbon sequestration–a sustainable solution to crop-residue burning in India. RSC Adv. 8 (1), 508–520.
Naghdi, M., Taheran, M., Brar, S.K., Kermanshahi-Pour, A., Verma, M., Surampalli, R.Y., 2017. Immobilized laccase on oxygen functionalized nanobiochars through mineral acids treatment for removal of carbamazepine. Sci. Total Environ. 584, 393–401.
Naghdi, M., Taheran, M., Pulicharla, R., Rouissi, T., Brar, S.K., Verma, M., Surampalli, R. Y., 2019. Pine-wood derived nanobiochar for removal of carbamazepine from aqueous media: adsorption behavior and influential parameters. Arab. J. Chem. 12 (8), 5292–5301.
Najafian, M., Kafilzadeh, F., Azad, H.N., Tahery, Y., 2012. Toxicity of chromium ($Cr6+$) on growth, ions and some biochemical parameters of *Brassica napus* L. Am.-Eurasian J. Agric. Environ. Sci. 12 (2), 237–242.
Nakano, Y., Asada, K., 1981. Hydrogen peroxide is scavenged by ascorbate-specific peroxidase in spinach chloroplasts. Plant Cell Physiol. 22 (5), 867–880.
Pavesi, T., Moreira, J.C., 2020. Mechanisms and individuality in chromium toxicity in humans. J. Appl. Toxicol. 40 (9), 1183–1197.
Pavia, D.L., Lampman, G.M., Kriz, G.S., Vyvyan, J.A., 2014. Introduction to spectroscopy. Cengage learning.
Peng, H., Chen, Y., Weng, L., Ma, J., Ma, Y., Li, Y., Islam, M.S., 2019. Comparisons of heavy metal input inventory in agricultural soils in North and South China: a review. Sci. Total Environ. 660, 776–786.
Peterson, S.C., Jackson, M.A., Kim, S., Palmquist, D.E., 2012. Increasing biocar surface area: optimization of ball miling parameters. Powder Technol. 22, 115–120. https://doi.org/10.1016/j.powtec.2012.05.005.
Rai, V., Khatoon, S., Rawat, A.K.S., Mehrotra, S., 2007. Disruption of elements uptake due to excess chromium in Indian medicinal plants. Biol. Trace Elem. Res. 120 (1), 127–132.
Rajapaksha, A.U., Vithanage, M., Ok, Y.S., Oze, C., 2013. Cr (VI) formation related to Cr (III)-muscovite and birnessite interactions in ultramafic environments. Environ. Sci. Technol. 47 (17), 9722–9729.
Rajasekhar, S., Kuldeep, B., 2011. A Review-Pahrmacognosy and pharmacology of *Nigella sativa*. Int. Res. J. Pharm. 2 (11), 36–39.
Ramzan, M., Ayub, F., Shah, A.A., Naz, G., Shah, A.N., Malik, A., Abd Elgawad, H., 2022. Synergistic effect of zinc oxide nanoparticles and *Moringa oleifera* leaf extract alleviates cadmium toxicity in *Linum usitatissimum*: antioxidants and physiochemical studies. Front. Plant Sci. 13.
Ramzani, P.M.A., Coyne, M.S., Anjum, S., Iqbal, M., 2017. In situ immobilization of Cd by organic amendments and their effect on antioxidant enzyme defense mechanism in mung bean (*Vigna radiata* L.) seedlings. Plant Physiol. Biochem. 118, 561–570.
Siara, S., Mayara, G.G., Paulo, A.S.V., Tassya, T.S.M., Patricio, P.Z., Antonio, S.M., 2019. TiO2 supported on Salvinia molesta biochar for heterogeneous photocatalytic degradation of Acid Orange 7 dye. J. Environ. Chem. Eng. 7 (1), 102879.
Saxena, M., Maity, S., Sarkar, S., 2014. Carbon nanoparticles in 'biochar'boost wheat (*Triticum aestivum*) plant growth. Royal society of chemistry Advances 4 (75), 39948–39954.
Shahbaz, A.K., Iqbal, M., Jabbar, A., Hussain, S., Ibrahim, M., 2018a. Assessment of nickel bioavailability through chemical extractants and red clover (*Trifolium pratense* L.) in an amended soil: related changes in various parameters of red clover. Ecotoxicol. Environ. Saf. 149, 116–127.
Shahbaz, A.K., Lewińska, K., Iqbal, J., Ali, Q., Iqbal, M., Abbas, F., Ramzani, P.M.A., 2018b. Improvement in productivity, nutritional quality, and antioxidative defense mechanisms of sunflower (*Helianthus annuus* L.) and maize (*Zea mays* L.) in nickel contaminated soil amended with different biochar and zeolite ratios. Journal of environmental management 218, 256–270.
Shahid, M., Shamshad, S., Rafiq, M., Khalid, S., Bibi, I., Niazi, N.K., Rashid, M.I., 2017. Chromium speciation, bioavailability, uptake, toxicity and detoxification in soil-plant system: a review. Chemosphere 178, 513–533.
Shannon, L.M., Kay, E., Lew, J.Y., 1966. Peroxidase isozymes from horseradish roots: I. Isolation and physical properties. J. Biol. Chem. 241 (9), 2166–2172.
Sial, T.A., Lan, Z., Wang, L., Zhao, Y., Zhang, J., Kumbhar, F., Shah, A.N., 2019. Effects of different biochars on wheat growth parameters, yield and soil fertility status in a silty clay loam soil. Molecules 24 (9), 1798.
Singh, D., Sharma, N., 2017. Effect of chromium on seed germination and seedling growth of green garm (*Phaseols Aureus* L) and chickpea (*Cicer Arietinum* L). Int. J. Appl. Nat. Sci. 6, 37–46.
Sinha, A.K., 1972. Colorimetric assay of catalase. Anal. Biochem. 47 (2), 389–394.
Srivastava, D., Tiwari, M., Dutta, P., Singh, P., Chawda, K., Kumari, M., Chakrabarty, D., 2021. Chromium stress in plants: toxicity, tolerance and phytoremediation. Sustainability 13 (9), 4629.
Stambulska, U.Y., Bayliak, M.M., Lushchak, V.I., 2018. Chromium (VI) Toxicity in Legume Plants: Modulation Effects of Rhizobial Symbiosis. BioMed research international, 2018.
Sulaiman, G.M., Mohammed, W.H., Marzoog, T.R., Al-Amiery, A.A.A., Kadhum, A.A.H., Mohamad, A.B., 2013. Green synthesis, antimicrobial and cytotoxic effects of silver nanoparticles using *Eucalyptus chapmaniana* leaves extract. Asian Pac. J. Trop. Biomed. 3 (1), 58–63.
Tripathi, S., Sonkar, S.K., Sarkar, S., 2011. Growth stimulation of gram (*Cicer arietinum*) plant by water soluble carbon nanotubes. Nanoscale 3 (3), 1176–1181.
Turan, V., Ramzani, P.M.A., Ali, Q., Abbas, F., Iqbal, M., Irum, A., Khan, W.U.D., 2018. Alleviation of nickel toxicity and an improvement in zinc bioavailability in sunflower seed with chitosan and biochar application in pH adjusted nickel contaminated soil. Arch. Agron Soil Sci. 64 (8), 1053–1067.
Usman, K., Al Jabri, H., Abu-Dieyeh, M.H., Alsafran, M.H., 2020. Comparative assessment of toxic metals bioaccumulation and the mechanisms of chromium (Cr) tolerance and uptake in *Calotropis procera*. Front. Plant Sci. 11, 883.
Vivas, A., Barea, J.M., Biró, B., Azcón, R., 2006. Effectiveness of autochthonous bacterium and mycorrhizal fungus on Trifolium growth, symbiotic development and soil enzymatic activities in Zn contaminated soil. J. Appl. Microbiol. 100 (3), 587–598.
Wang, D., Zhang, W., Hao, X., Zhou, D., 2013. Transport of biochar particles in saturated granular media: effects of pyrolysis temperature and particle size. Environ. Sci. Technol. 47 (2), 821–828.
Wang, S., Chen, F., Mu, S., Zhang, D., Pan, X., Lee, D.J., 2013. Simultaneous analysis of photosystem responses of *Microcystis aeruginoga* under chromium stress. Ecotoxicol. Environ. Saf. 88, 163–168.
Willis, A.J., Yemm, E.W., 1955. The micro-estimation of sugars in plant tissues. New Phytol. 54 (3), 289–291.
Yimer, E.M., Tuem, K.B., Karim, A., Ur-Rehman, N., Anwar, F., 2019. *Nigella sativa* L. (black cumin): a promising natural remedy for wide range of illnesses. Evid. base Compl. Alternative Med. 2019.
Yu, J.T., Dehkhoda, A.M., Ellis, N., 2011. Development of biochar-based catalyst for transesterification of canola oil. Energy Fuels 25 (1), 337–344.
Yue, L., Lian, F., Han, Y., Bao, Q., Wang, Z., Xing, B., 2019. The effect of biochar nanoparticles on rice plant growth and the uptake of heavy metals: implications for agronomic benefits and potential risk. Sci. Total Environ. 656, 9–18.
Zhao, M., Xu, J., Li, A., Mei, Y., Ge, X., Liu, X., Xu, Q., 2020. Multiple exposure pathways and urinary chromium in residents exposed to chromium. Environ. Int. 141, 105753.
Zheng, H., Wang, X., Chen, L., Wang, Z., Xia, Y., Zhang, Y., Xing, B., 2018. Enhanced growth of halophyte plants in biochar-amended coastal soil: roles of nutrient availability and rhizosphere microbial modulation. Plant Cell Environ. 41 (3), 517–532.